NASA Technical Memorandum 82800

Hydrodynamic and Aerodynamic Breakup of Liquid Sheets

R. Ingebo
Lewis Research Center
Cleveland, Ohio

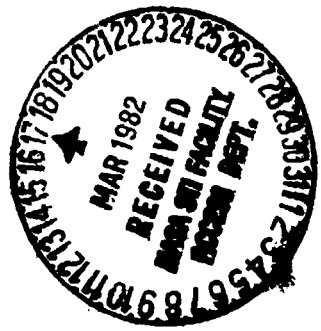

Prepared for the
Second International Conference on Liquid Atomization and Spray Systems
sponsored by the University of Wisconsin
Madison, Wisconsin, June 20–24, 1982

NASA

Hydrodynamic and Aerodynamic Breakup of Liquid Sheets

R. Ingebo

NASA Lewis Research Center
Cleveland, Ohio

ABSTRACT

Hydrodynamic and aerodynamic breakup of water sheets into sprays formed by impinging jet, splash plate and conventional simplex fuel nozzles were investigated in quiescent air and high velocity airstreams. Mean drop diameter D_m for each spray was determined with a scanning radiometer previously developed at NASA Lewis Research Center. With impinging jet fuel injectors, the ratio of orifice diameter D_o to mean drop diameter D_m was correlated with hydrodynamic force in terms of the liquid jet Reynolds number Re_l and aerodynamic force in terms of the airstream relative velocity Reynolds number Re_r as follows: $D_o/D_m = 0.023\ Re_l^{0.5} + 2\times10^{-3}\ Re_r$. With high velocity airstreams, aerodynamic force contributed the most to breakup since $Re_r >> Re_l$. Liquid sheet breakup with splash plate fuel injectors gave the following expression: $D_o/D_m = 2.6\times10^{-4}\ Re_l + 2.4\times10^{-3}\ Re_a$ where Re_a is airstream Reynolds number based on airstream velocity. Hydrodynamic force was much more effective in breakup with splash plates than with impinging jet fuel injectors since D_o/D_m varied with Re_l to the first power. Breakup of swirling water sheets formed with simplex pressure atomizing fuel nozzles gave the following expression: $D_o/D_m = D_o/D_{m,h} + 2.2\times10^{-3}\ (Re_a - Re_c)$ where $D_{m,h}$ and Re_c are constants defined as the hydrodynamic mean drop diameter and the critical Reynolds number for aerodynamic breakup, respectively. Hydrodynamic force was considerably more effective in breakup with swirling sheets than with splash plate fuel injectors. However, aerodynamic force tended to decrease the cone angle and increase mean drop size with airstream Reynolds numbers below the critical Reynolds number Re_c. Experimental conditions included water flow rates of 27 to 68 liter per hour and airflow mass velocities of 1.7 to 25.7 g/cm^2 - sec at 293 K and atmospheric pressure.

E-1139

NOMENCLATURE

D	diameter, cm
D_m	experimental mean drop diameter, cm
D_{30}	volume-number mean drop diameter, $(\Sigma nD_d^3/\Sigma n)^{0.33}$, cm
D_{32}	Sauter mean diameter, $\Sigma nD_d^3/\Sigma nD_d^2$, cm
Fn	flow number, $L/hr(N/m^2)^{0.5}$
k	coefficient
ΔP	liquid differential pressure, N/m^2
Re_a	airstream Reynolds number, D_oV_a/ν_a
Re_c	constant
Re_l	liquid jet Reynolds number, D_oV_l/ν_l
Re_r	airstream relative velocity Reynolds number, D_oV_r/ν_a
V	velocity, cm/sec
μ	absolute viscosity, g/cm-sec
ν	kinematic viscosity, cm^{2}sec
ρ	dersity, g/cm^3

Subscripts:

a	airstream
c	critical
d	droplet
l	liquid
m	mean
o	orifice
r	relative

INTRODUCTION

An investigation was conducted to study the interaction and determine the effect of hydrodynamic, aerodynamic and liquid surface forces on the mean drop diameter of water sprays that are produced by the breakup of nonswirling and swirling water sheets in quiescent air and in airflows similar to those encountered in gas turbine combustors. The mean drop diameter is used to characterize fuel sprays and it is a very important factor in determining the performance and exhaust emissions of gas turbine combustors. This is demonstrated in Ref. 1 where nitrogen oxide emissions in the exhaust gases

were found to vary directly with the square of the mean drop diameter of the fuel spray.

Several investigators have studies the atomization of liquid jets in airstream. In Ref. 2, Mayer identifies capillary-wave breakup as occurring when relatively large liquid jets are injected in quiescent or very low velocity airstreams. In this case, hydrodynamic and aerodymanic forces are relatively low. However, when the velocity of the airstream relative to the liquid jet velocity is large and the aerodynamic force is sufficiently high, then according to Adelberg in Ref. 3 another type of breakup occurs which he defines as acceleration-wave breakup. In Ref. 4 it was found that the mean drop diameter for liquid jet breakup could be correlated with the product of the Weber and Reynolds number, and transition from capillary to acceleration wave breakup occurred when the value of the product of the Weber and Reynolds number equaled 10^6.

In the present study of liquid sheet atomization, the effect of hydrodynamic and aerodynamic force on mean drop diameter was studied in the regimes of capillary-wave and acceleration-wave breakup. Three general conditions of liquid sheet atomization were investigated, namely, breakup in quiescent air, in airstream of zero velocity relative to liquid jet velocity, and in high velocity airstreams. In the first case, i.e. liquid sheet breakup in quiescent air, both hydrodynamic and aerodynamic forces interact with liquid forces, and atomization generally occurs in the capillary wave breakup regime. In the second case, only hydrodynamic forces appreciably effect the mean drop diameter since aerodynamic force is negligible. Breakup is primarily in the capillarywave regime and as a result mean drop diameters are larger than those obtained with quiescent air. In the final case of liquid sheet breakup in high velocity airstreams, the aerodynamic force has the major effect on fineness of atomization and breakup occurs primarily in the acceleration-wave regime. This condition is most applicable to gas turbine combustors operating at idle, take-off and cruise conditions.

Non-swirling and swirling liquid sheets were injected in airstreams and mean drop diameter data were obtained from water sprays produced by impinging jet, splash plate and conventional simplex pressure atomizing fuel nozzles. Non-swirling liquid sheets were injected axially and radially in airstreams and swirling hollow-cone sheets were injected at a cone-angle of 45° in quiescent and non-swirling airflows in a 7.6 cm. inside diameter duct. The airstream mass velocity, $\rho_a V_a$, was varied from 1.5 to 25.7 g/cm^2-sec at 293 K and atmospheric pressure. Orifice diameters varied from 0.033 to 0.212 cm for the three different types of fuel injectors. Water flow rates were varied from 27 to 68 liter per hour. Mean drop diameter data were then correlated with hydrodynamic forces based on liquid velocity and orifice diameter and with aerodynamic forces based on airstream mass velocity.

APPARATUS AND PROCEDURE

Fuel injectors were mounted in the open-duct facility as shown in Fig. 1. Airflow was drawn from the laboratory supply system, at ambient temperature (293 K) as determined with an I.C. thermocouple, and exhausted into the atmosphere. Airflow rate was determined with an orifice as the airflow control valve was opened until the desired airflow rate per unit area was obtained over a mass velocity range of 1.7 to 25.7 g/cm^2-sec. The bellmouth test section shown in Fig. 1 has a total length of 15.2 cm, an inside diameter (of the circular duct) of 7.6 cm and it is mounted inside of a duct that is 5 m in length with an inside diameter of 15.2 cm.

Water sheets were produced at the duct center line and directed axially downstream with the fuel injectors shown in Figs. 2(a) to (c). The impinging jets produced a relatively flat sheet flowing in the same direction as the airflow. The splash plate produced a liquid sheet injected radially or normal to the airflow, and the conventional Monarch simplex nozzle produced a swirling hollow-cone sheet with a cone-angle of 45° in quiescent air, i.e. no airflow in the duct. The water sheets, at 293 K as determined with an I.C. thermocouple, were formed by gradually opening a water flow control valve until the desired water flow rate over a range of 27 to 68 liters/hour was obtained as measured with a turbine flow meter.

When the air and water flow rates were set, mean drop diameter data were obtained with the scanning radiometer mounted 11.4 cm downstream of the open-duct exit. The scanning radiometer optical system shown in Fig. 3 consisted of a 1-milliwatt helium-neon laser, a 0.003-cm-diam aperature, a 7.5-cm-diam collimating lens, a 10-cm-diam converging lens, a 5-cm-diam collecting lens, a scanning disk with a 0.05- by 0.05-cm slit, a timing light, and a photomultiplier detector. A more complete description of the scanning radiometer, the mean drop diameter range, and the method of determining mean particle size are discussed in Refs. 5 and 6.

EXPERIMENTAL RESULTS

To obtain a better understanding of liquid sheet atomization and thereby advance fuel injector technology for gas turbine combustor and augmentor applications, mean drop diameters were determined for the breakup of water sheets in high velocity airstreams. Axially and radially injected sheets were produced with impinging jet and splash plate fuel injectors, respectively. Swirling hollow-cone sheets were injected axially downstream with pressure atomizing simplex nozzles.

Impinging Jet Fuel Injectors

The effect of airstream relative mass velocity $\rho_a V_r$ on the reciprocal mean drop diameter D_m^{-1} is shown in Fig. 4 and the following expression is obtained:

$$D_m^{-1} = 0.23\,(V_l D_o)^{0.5} + 11\,\rho_a V_r \qquad (1)$$

where V_l and V_r are liquid velocity and airstream velocity relative to the liquid velocity, respectively. This expression may be rewritten in terms of the dimensionless ratio of orifice to mean drop diameter D_o/D_m, the liquid jet Reynolds number Re_l for hydrodynamic breakup, and the airstream relative velocity Reynolds number Re_r for aerodynamic breakup as follows:

$$\frac{D_o}{D_m} = 23\times10^{-3}\,Re_l^{0.5} + 2.0\times10^{-3}\,Re_r \qquad (2)$$

since $\nu_l = 10.1\times10^{-3}$ cm^2/sec and $\mu_a = 1.81\times10^{-4}$ g/cm-sec. The mean drop diameter D_m

measured with the scanning radiometer is assumed to be approximately equal to the Sauter mean diameter, SMD or D_{32}.

The effect of mass velocity $\rho_a V_a$ on D_m is shown in Fig. 5. This plot gives a better overall picture of liquid sheet breakup and shows that the reciprocal mean drop diameter for hydrodynamic breakup, $D_{m,h}^{-1}$, is equal to 110 and 10 for the 0.033 and 0.212 centimeter-diameter orifices, respectively. This occurs when $V_a = V_l$ and therefore $V_r = 0$. Also, Fig. 8 shows that when the data are extrapolated to the condition $V_a = 0$, then $D_{m,h}$ is equal to 210 and 20 for the 0.033 and 0.212 centimeter-diameter orifices, respectively.

Similar relationships for the breakup on n-heptane sheets produced with impinging jet fuel injectors for rocket combustors are derived in the Appendix. The derivation is based on mean drop size data given in Ref. 7 which were obtained with a photographic technique. As a result, the following expression is derived in terms of the Sauter mean drop diameter D_{32} as follows:

$$\frac{D_o}{D_{32}} = 18.6\times10^{-3}\ Re_l^{0.5} + 1.55\times10^{-3}\ Re_a \qquad (3)$$

Comparison of Eq. (3) with Eq. (2) shows that the hydrodynamic breakup coefficient of 23.0×10^{-3} for water sprays is somewhat higher than that of 18.6×10^{-3} for n-heptane sprays. Also, the aerodynamic breakup coefficient of 2×10^{-3} for water sprays is somewhat larger than that for n-heptane sprays. This may be attributed to the fact that Eq. (2) is obtained for very high momentum airstreams with a mass velocity, $\rho_a V_a$, range of 7.3 to 25.7 g/cm^2-sec which is primarily in the acceleration-wave breakup regime. Equation (3), as derived from Ref. 7, only covers a mass velocity range of 2.4 to 11 g/cm^2-sec which is primarily in the capillary-wave breakup regime for low momentum airstreams.

Splash Plate Fuel Injectors

Breakup in airstreams of radially injected water sheets produced by the splash plate fuel injector shown in Fig. 3 was investigated. As shown in Figs. 6(a) and (b), values of D_m are plotted against mass velocity, $\rho_a V_a$, for the 0.1016 and 0.216 centimeter-diameter fuel tubes, respectively. Mean drop diameter data for D_m^{-1} give the following empirical relation:

$$D_m^{-1} = D_{m,o}^{-1} + 13\ \rho_a V_a \qquad (4)$$

where $D_{m,o}^{-1}$ is the value of D_m^{-1} at $V_r = V_a = 0$. Since breakup data for the condition $V_a = 0$ was not obtained for the splash plate fuel injector, values of $D_{m,o}^{-1}$ were determined by extrapolating the data to $V_a = 0$. These values are then plotted against liquid jet velocity, V_l, as shown in Fig. 7 to give the following expression:

$$D_{m,o}^{-1} = 0.028\ V_l \qquad (5)$$

for the hydrodynamic and aerodymanic breakup of water sheets in quiescent air, i.e. $V_a = 0$. At this condition, D_m^{-1} is directly proportional to the liquid jet velocity and independent or orifice diameter. This result is quite different from that obtained with impinging jets. Thus, the two expressions, Eq. (7) and Eq. (1) can not be compared directly since the first term on the right hand side of Eq. (1) is derived strictly for hydrodynamic breakup whereas $D_{m,o}^{-1}$ includes both hydrodynamic and aerodynamic breakup.

By substituting Eq. (5) into Eq. (4), the following expression for splash plate fuel injector breakup of water sheets in high velocity airstreams is obtained:

$$D_m^{-1} = 0.028\ V_l + 13\ \rho_a V_a \qquad (6a)$$

which may be rewritten as follows:

$$\frac{D_o}{D_m} = 2.8\times10^{-4}\ Re_l + 2.4\times10^{-3}\ Re_a \qquad (6b)$$

Comparison of equation 6b for splash plate fuel injectors with Eq. (2) for impinging jets shows that hydrodynamic breakup varies with Re_l to the first power in equation 6b and with $Re_l^{0.5}$ in Eq. (2). However, the coefficient for Re_l is considerably higher in Eq. (2) than Eq. (6b). Data from Fig. 5 for impinging jets are plotted in Fig. 6(b) for comparison and show that values of D_m^{-1} were somewhat lower for impinging jets of approximately the same orifice diameter of 0.216 centimeters.

Pressure Atomizating Simplex Nozzles

Breakup of swirling hollow-cone water sheets injected axially downstream in high momentum airflows was investigated. This is a much more complicated type of liquid sheet breakup to analyze due to the difficulty of establishing the velocity of the swirling liquid relative to the airstream, i.e. V_r. Also, the effect of airstream mass velocity on varying and reducing the cone angle obtained with various sizes of simplex nozzles adds to the difficulties of determining V_r. Thus, for this study, D_m^{-1} data are plotted against mass velocity, $\rho_a V_a$, as shown in Fig. 8.

At the initial condition, $\rho_a V_a = 0$ and $D_m^{-1} = D_{m,o}$. Both hydrodynamic and aerodynamic forces are affecting the liquid sheet breakup process. However, as mass velocity, $\rho_a V_a$, is increased the value of D_m^{-1} decreased until it reaches a minimum value of $D_{m,h}^{-1}$ since relative velocity, V_r, approaches zero and the breakup process is primarily controlled by the hydrodynamic pressure drop of the liquid. As mass velocity is increased from 4 to 14.5 g/cm^2-sec for the small nozzles ($D_o = 0.09$) there is only a slight increase in D_m^{-1}. This intermediate region is primarily a capillary-wave breakup regime which is transformed into acceleration-wave breakup as mass velocity is increased to the maximum value of 25.7 g/cm^2-sec. Thus, the following empirical expressions are derived from the data plotted in Fig. 8:

$$D_m^{-1} = D_{m,h}^{-1} + 12\ (\rho_a V_a - \rho_c V_c) \qquad (7a)$$

which may be rewritten as:

$$\frac{D_o}{D_m} - \frac{D_o}{D_{m,h}} = 2.2\times10^{-3}\,(Re_a - Re_c) \qquad (7b)$$

where $D_{m,h}$ = 210 and 140 cm when D_o = 0.09 and 0.13 cm respectively, and $\rho_c V_c$ = 14.5 and 11.5 g/cm^2-sec when D_o = 0.09 and 0.13 cm, respectively.

It is interesting to note that low momentum airstreams, with values of $Re_a < Re_c$ and mass velocities below 20 g/cm^2-sec, tended to give values of D_m^{-1} which were below the values obtained in quiescent air. This is attributed to a decrease in cone angle of the hollow-cone spray which produces larger drop sizes and less efficient atomization, and a decrease in relative velocity V_r. It was only by going to values of $\rho_a V_a$ 20 g/cm^2-sec that drop size was decreased and values of D_m^{-1} or specific surface area of the spray was appreciably increased.

Figure 8 also includes a plot of the data from Figure 6a for the splash plate fuel injector that has an orifice diameter of 0.1016 centimeters. At high mass velocities the splash plate gave much better breakup, i.e. a higher value of D_m^{-1}, than the simplex nozzle having an orifice diameter of 0.08 centimeters. The lower value of the simplex nozzle may be caused by the collapse of the spray cone angle. However, a comparison of Eq. (7b) with Eqs. (5) and (6b) shows that a coefficient of 2.2×10^{-3} was obtained for aerodynamic breakup in the acceleration-wave regime which is approximately the same value as that obtained for the impinging jet and splash plate fuel injectors. In the case of injection into quiescent air, Fig. 8 shows that hydrodynamic breakup with simplex nozzles is much more effective in producing finely atomized sprays that the splash plate or impinging jet fuel injector.

Values of $D_{m,o}^{-1}$ for quiescent air (V_a = 0) are plotted against liquid differential pressure, ΔP on the log log plot shown in Fig. 9 which gives the following expression:

$$D_m^{-1} = k\,\Delta P_l^{0.30} \qquad (8)$$

where the coefficient k is a constant for a given simplex fuel nozzle. By assuming $D_{m,o}^{-1}$ to be a function of the nozzle flow number Fn, the coefficient k is evaluated to give the following correlating expression for the two simplex fuel nozzles:

$$D_{m,o} = 0.73\,Fn^{-0.34}\,\Delta P^{0.30} \qquad (9)$$

where ΔP and Fn are expressed in N/m^2 and l/hr (N/m^2)$^{0.5}$, respectively.

In Ref. 7, the following expression was obtained for kerosene sprays and the condition V_a = 0:

$$D_{32,o} = 0.74\,Fn^{-0.34}\,\Delta P^{0.27} \qquad (10)$$

Mean drop diameters were obtained with a light scattering instrument and kerosene sprays were produced with simplex Delavan nozzles having a cone angle of 80° and flow numbers ranging from 0.0182 to 0.0364. Comparison of Eqs. (9) and (10) shows exponents for the flow number and ΔP agree very well. Also, the coefficients in the two equations are approximately the same. However, the coefficients can not be compared directly since Eq. (9) was derived in this study for simplex Monarch nozzles producing water sprays at a cone angle of 45° in quiescent air.

SUMMARY OF RESULTS

Empirical correlations of the ratio of orifice diameter D_o to mean drop diameter D_m with hydrodynamic force in terms of the liquid jet Reynolds number Re_l and aerodynamic force in terms of the airstream Reynolds number Re_a or the airstream relative velocity Reynolds number Re_r were derived in this investigation of liquid sheet breakup in non-swirling airflow. They are listed as follows:

1. Impinging jet fuel injectors gave the empirical relationship, $D_o/D_m = 0.023\,Re_l^{0.5} + 2\times10^{-3}\,Re_r$ and with high velocity airstream, aerodynamic force contributed the most to breakup since $Re_r >> Re_l$

2. Splash plate fuel injectors gave the empirical relationship, $D_o/D_m = 2.9\times10^{-4}\,Re_l + 2.4\times10^{-3}\,Re_a$ and hydrodynamic force was much more effective in breakup with splash plates than with impinging jet fuel injectors since D_o/D_m varied with Re_l to the first power.

3. Simplex pressure atomizing fuel nozzles gave the empirical relationship, $D_o/D_m = D_o/D_{m,h} + 2.2\times10^{-3}\,(Re_a - Re_c)$ where $D_{m,h}$ and Re_c are constants defined as the hydrodynamic mean drop diameter and the critical Reynolds number for aerodynamic breakup, respectively. Hydrodynamic force was considerably more effective in breakup with swirling sheets than with splash plate fuel injectors. However, aerodynamic force tended to decrease the cone angle and increase mean drop size when airstream Reynolds numbers were below the critical Reynolds number Re_c.

APPENDIX

Liquid Sheet Atomization with Impinging Jet Fuel Injectors

In a previous experimental investigation described in Ref. 8, the breakup of n-heptane sheets axially injected in airstreams was studied. Mean drop diameter, D_{30}, data were obtained with a photographic technique for sprays produced by air-atomizing impinging-jet fuel injectors for rocket combustors. The effect of liquid pressure drop or hydrodynamic forces on the spray mean drop size was determined first. Then, the interacting or additive effect of hydrodynamic and aerodynamic forces on mean drop size was investigated.

Hydrodynamic Breakup

In Ref. 8, the following expression for the reciprocal mean drop diameter for hydrodynamic breakup, $D_{30,h}$, was obtained from a study of the breakup of pairs of impinging jets in airstreams with relative velocity $V_r = 0$ and $V_a = V_l$:

$$D_{30,h}^{-1} = 0.31\left(\frac{V_l}{D_o}\right)^{0.5} \qquad (11)$$

where V_l and D_o are the liquid jet velocity and orifice diameter respectively. A straight line

plot of Eq. (11) and the data for Ref. 8 are shown in Fig. 10. Equation 11 may be rewritten in terms of the dimensionless ratio of orifice diameter to hydrodynamic mean drop diameter, $D_{30,h}$, as follows:

$$\frac{D_o}{D_{30,h}} = 0.024\ Re_l^{0.5} \qquad (12)$$

since $Re_l = D_o V_l / \nu_l$ and $\nu_l = 0.0061$ cm^2/sec for n-heptane.

Aerodynamic Breakup

Data from Ref. 8 for aerodynamic breakup with hydrodynamic force held constant are plotted in Fig. 11 and give the following expression for mean drop size:

$$D_{30}^{-1} = 0.31\left(\frac{V_l}{D_o}\right)^{0.5} + 11\ \rho_a V_r \qquad (13)$$

where $\rho_a V_r$ is the relative mass velocity which produces the aerodynamic breakup of the liquid sheet. The usefulness of Eq. (13) is illustrated in Fig. 12 which shows, that initially when $V_a = 0$, the following expression is obtained: $D_{30,o}^{-1} = D_{30,h}^{-1} + 11\ \rho_a V_l$ since $D_{30,o}^{-1}$ is evaluated at $V_r = V_l$. Then as V_a increases V_r decreases until $V_r = 0$ and the value of D_{30}^{-1} decreased until $D_{30}^{-1} = D_{30,h}^{-1}$ as given by Eq. (11). Further increases in V_a increases V_r and values of D_{30}^{-1} increase as given by Eq. (13). The minimum value of D_{30}^{-1} at $V_r = 0$ is due to he negligible effect of aerodynamic force on breakup and illustrates the need of having mass velocities sufficiently high to more than compensate for the fuel velocity and obtain good fuel atomization in a combustor. Thus, $\rho_a V_a > 10$ is recommended when using impinging jet fuel injectors.

Equation (13) may be rewritten in terms of the dimensionless ratio D_o/D_{30} as follows:

$$\frac{D_o}{D_{30}} = 0.024\ Re_l^{0.5} + 2.0\times10^{-3}\ Re_a \qquad (14)$$

since $\rho_a = 1.81\times10^{-4}$ g/cm^3. In terms of the Sauter mean drop diameter D_{32}, the expression may be rewritten as follows:

$$\frac{D_o}{D_{32}} = 18.6\times10^{-3}\ Re_l^{0.5} + 1.55\times10^{-3}\ Re_a \qquad (15)$$

since $D_{32} = 1.29\ D_{30}$ as given in Ref. 9.

REFERENCES

[1] Ingebo, R. D. , "Atomizing Characteristics of Swirl Can Combustor Modules with Swirl Blast Fuel Injectors," NASA TM-79297, 1980.

[2] Mayer, E., "Capillary Mechanisms of Liquid Atomization in High Velocity Gas Streams," 12th International Astronautical Congress, Proceedings, Vol. 2, Academic Press, New York, 1963, pp. 731-740.

[3] Adelberg, M., "Mean Drop Size Resulting from the Injection of a Liquid Jet into a High-Speed Gas Stream," AIAA Journal Vol. 6, No. 6, June 1968, pp. 1143-1147.

[4] Ingebo, R. D., "Capillary and Acceleration Wave Breakup of Liquid Jets in Axial-Flow Air-streams," NASA TP-1791, 1981.

[5] Buchele, D. R., "Scanning Radiometer for Measurement of Forward-scattered Light to Determine the Mean Diameter of Spray Particles," NASA TM X-3454, 1976.

[6] Ingebo, R. D., "Effect of Airstream Velocity on Mean Drop Diameters of Water Sprays Produced by Pressure and Air Atomizing Nozzles," NASA TM-73740, 1977.

[7] Rao, K. V. L. and Lefebvre, A. H.: "Fuel Atomization in a Flowing Airstream," AIAA Journal, Vol. 13, No. 10, Oct. 1975, pp. 1413-1415.

[8] Ingebo, R. D., "Drop-Size Distributions for Impinging-Jet Breakup in Airstreams Simulating the Velocity Conditions in Rocket-Combustors," NACA TN-4222, 1957.

[9] Ingebo, R. D.: and Foster, H. H.: "Drop-Size Distribution for Crosscurrent Breakup of Liquid Jets in Airstreams", NACA TN-4087, 1957.

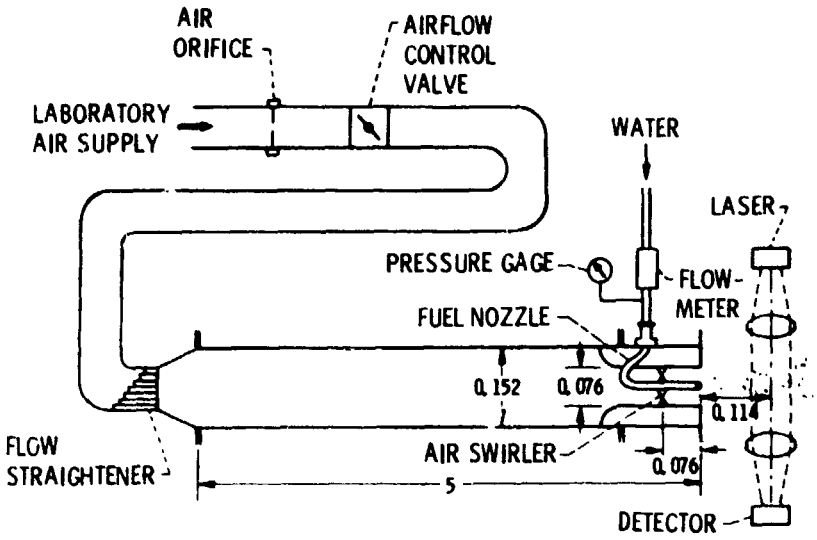

Figure 1. - Test facility and auxiliary equipment. (Dimensions are in meters.)

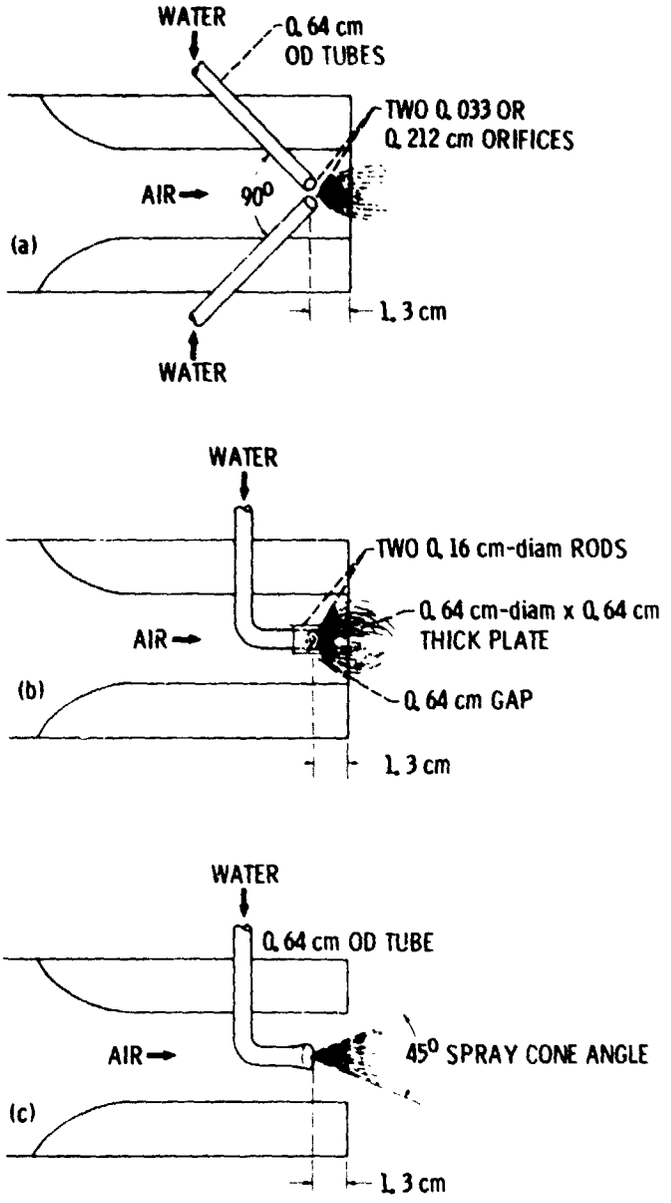

(a) Impinging jets with axially injected flat spray.

(b) Splash plate with radially injected flat spray.

(c) Simplex pressure atomizing nozzle with axially injected swirling hollow-cone spray.

Figure 2. - Liquid sheet fuel injectors.

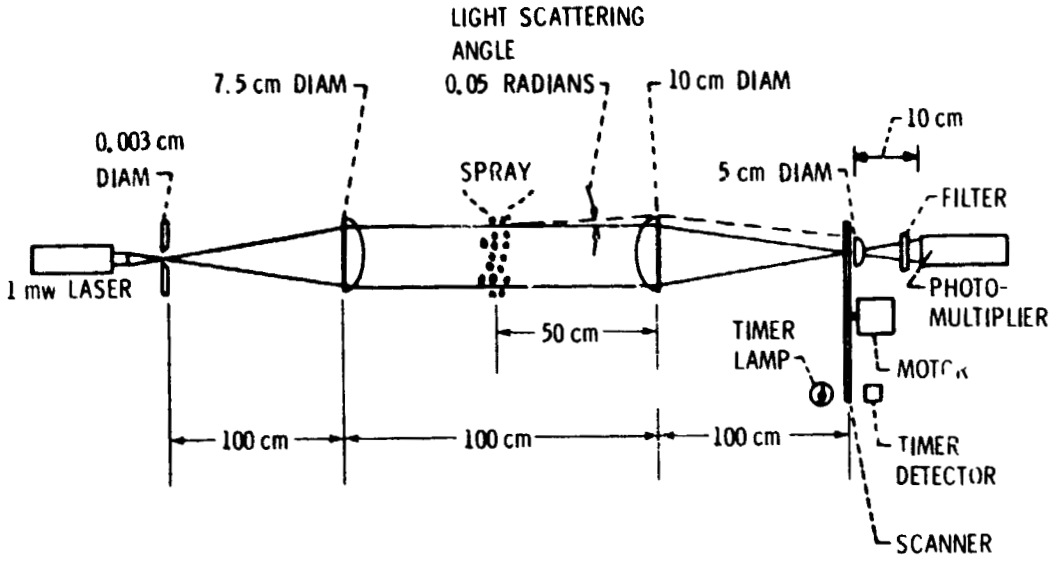

Figure 3. - Scanning radiometer optical path.

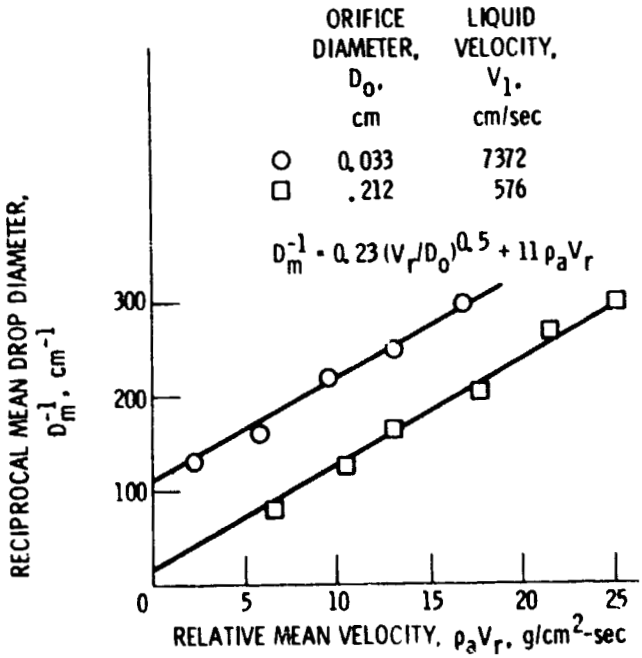

Figure 4. - Variation of reciprocal mean drop diameter, D_m^{-1}, with airstream relative mean velocity, $\rho_a V_r$, for water sheets produced by impinging jet injectors.

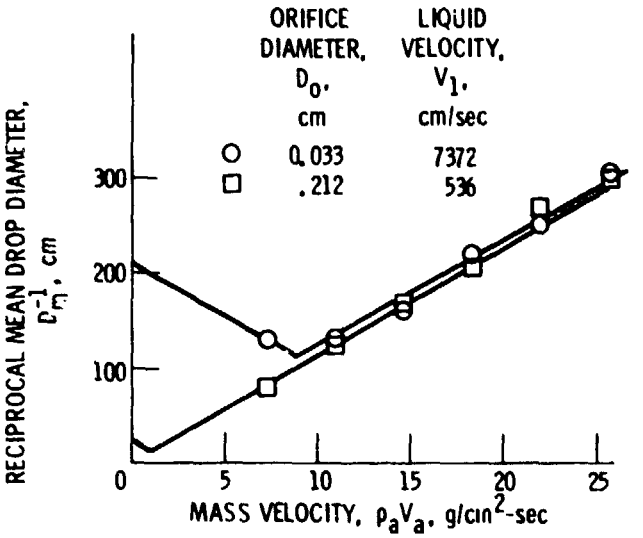

Figure 5. - Variation of reciprocal mean drop diameter, D_m^{-1}, with airstream mass velocity, $\rho_a V_a$, for water sheets produced by impinging jet fuel injectors.

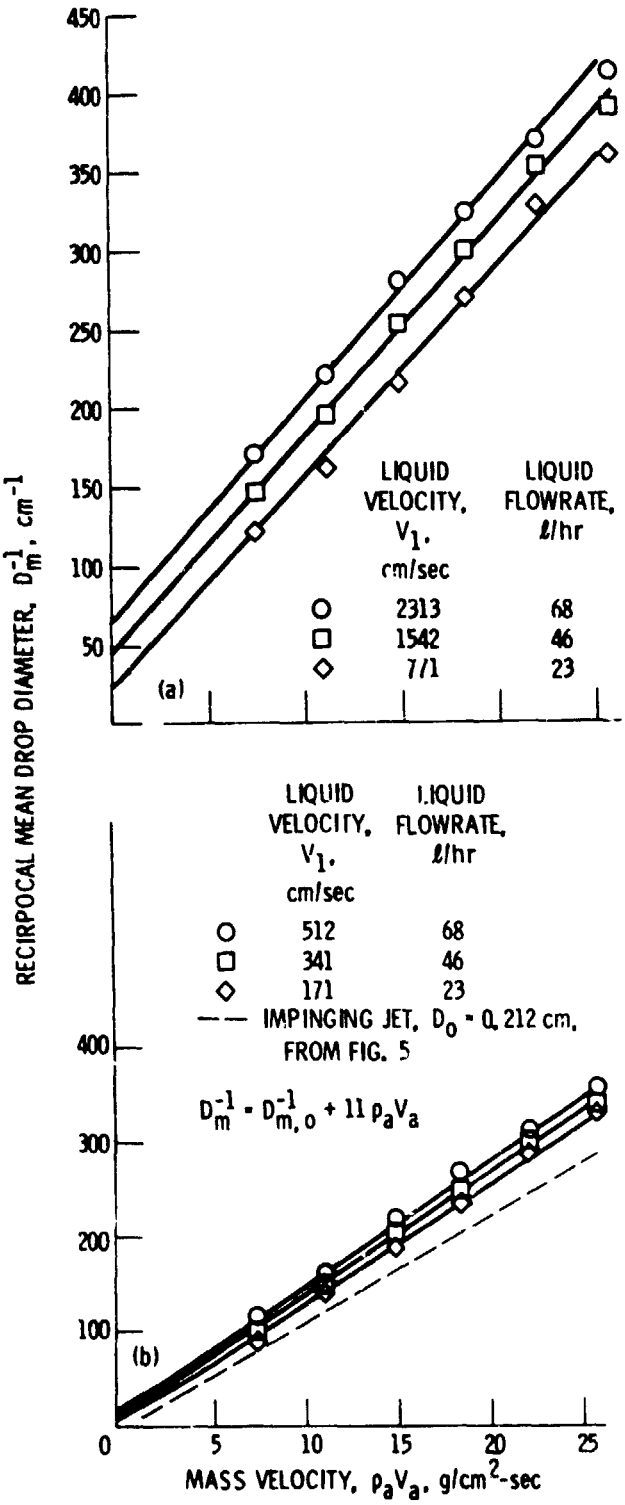

(a) 0.1016 cm-inside-diameter fuel tube.

(b) 0.216 cm-inside-diameter fuel tube.

Figure 6. - Variation of reciprocal mean drop diameter, D_m^{-1}, with airstream mass velocity for water sheets produced by splash plate fuel injector.

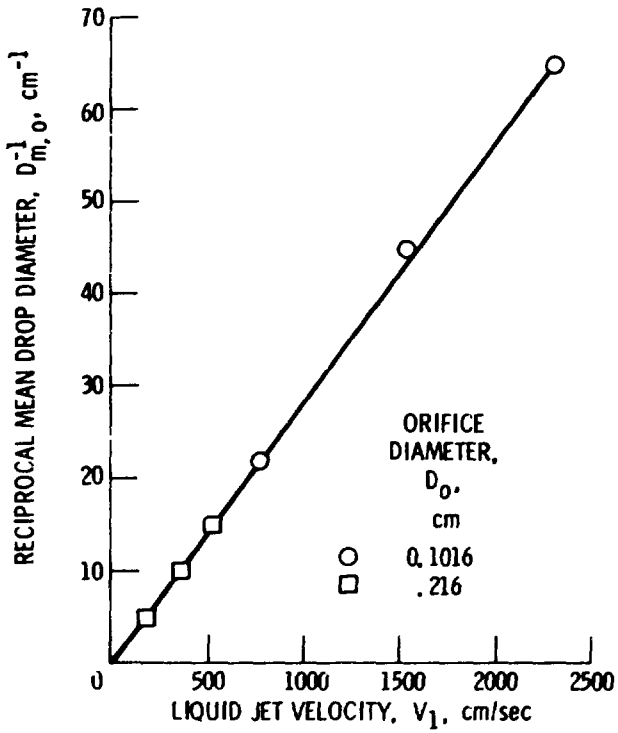

Figure 7. - Variation of reciprocal mean drop diameter, $D_{m,o}^{-1}$, with liquid jet velocity in quiescent air ($V_a = 0$) for water sheets produced by splash plate fuel injectors.

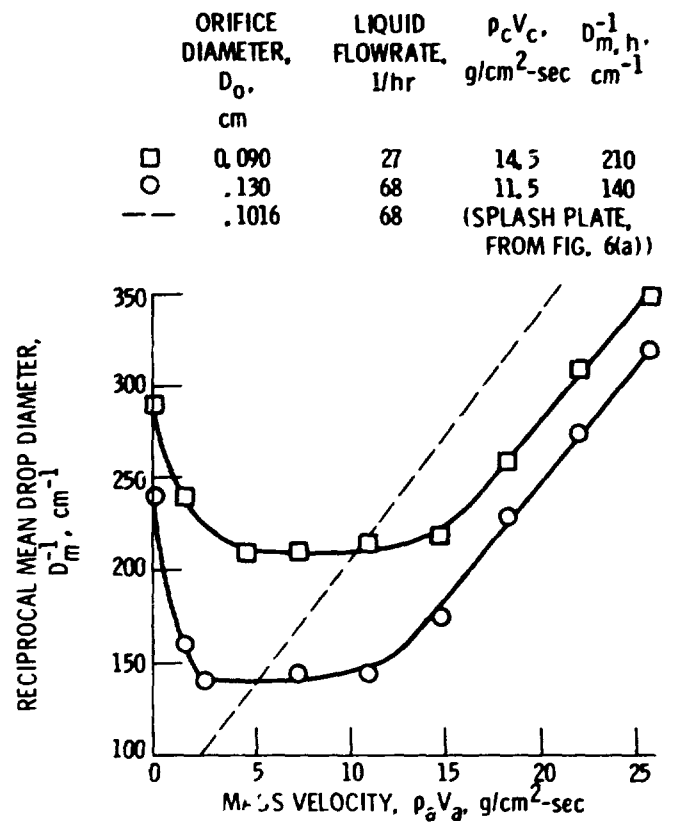

Figure 8. - Variation of reciprocal mean drop diameter, D_m^{-1}, with airstream mass velocity, $\rho_a V_a$, for swirling water sheets produced by simplex pressure atomizing nozzles.

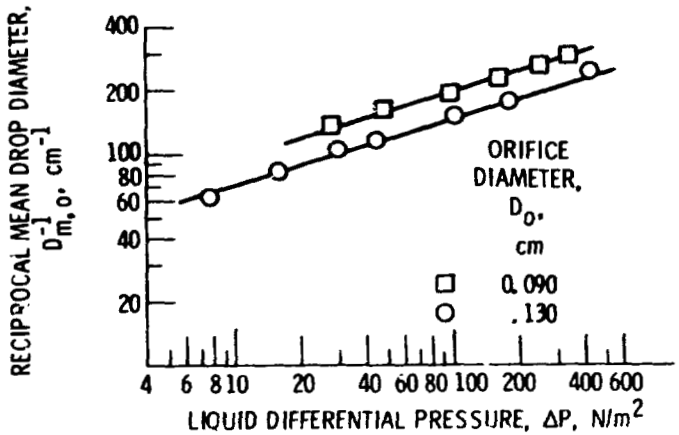

Figure 9. - Variation of reciprocal mean drop diameter, $D_{m,o}^{-1}$, with liquid differential pressure, ΔP, for swirling water sheets produced by simplex pressure atomizing nozzles.

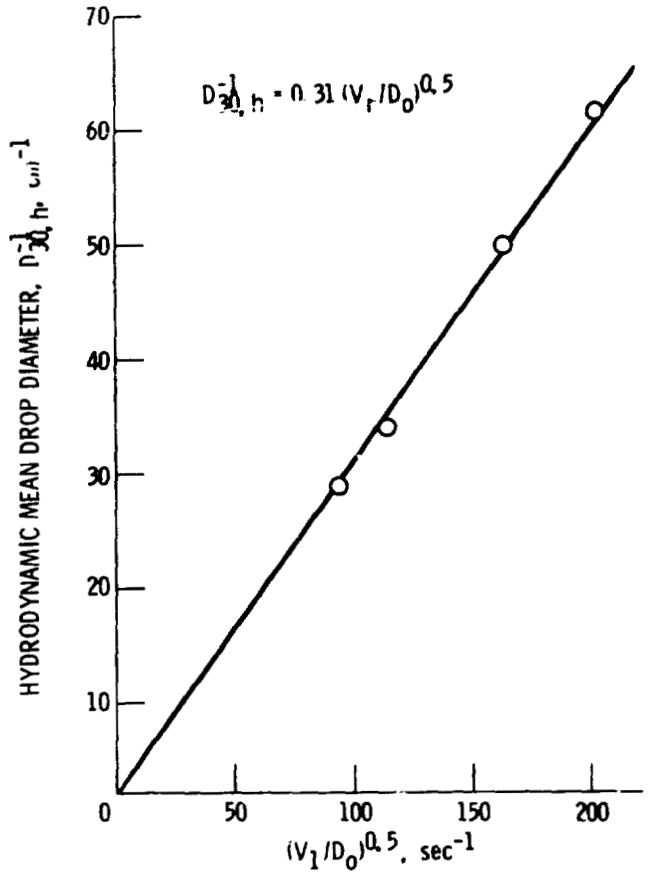

Figure 10. - Variation of hydrodynamic reciprocal mean drop diameter, $D_{30,h}^{-1}$, with square root ratio of liquid jet velocity to orifice diameter for n-heptane sheets produced by impinging jet fuel injectors, with $V_r = 0$ and $D_o = 0.74$ cm.

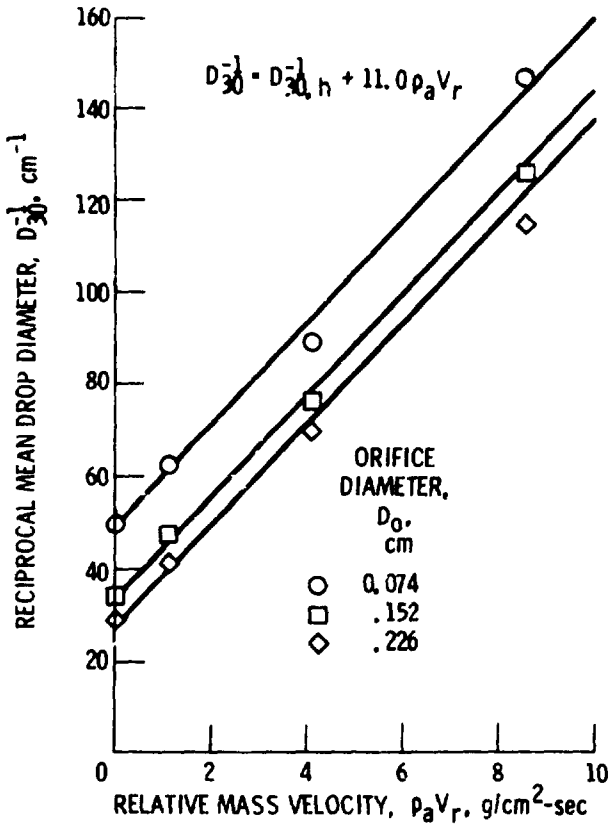

Figure 11. - Variation of reciprocal mean drop diameter, D_{30}^{-1}, with airstream relative mass velocity, $\rho_a V_r$, n-heptane sheets produced by impinging jet fuel injectors.

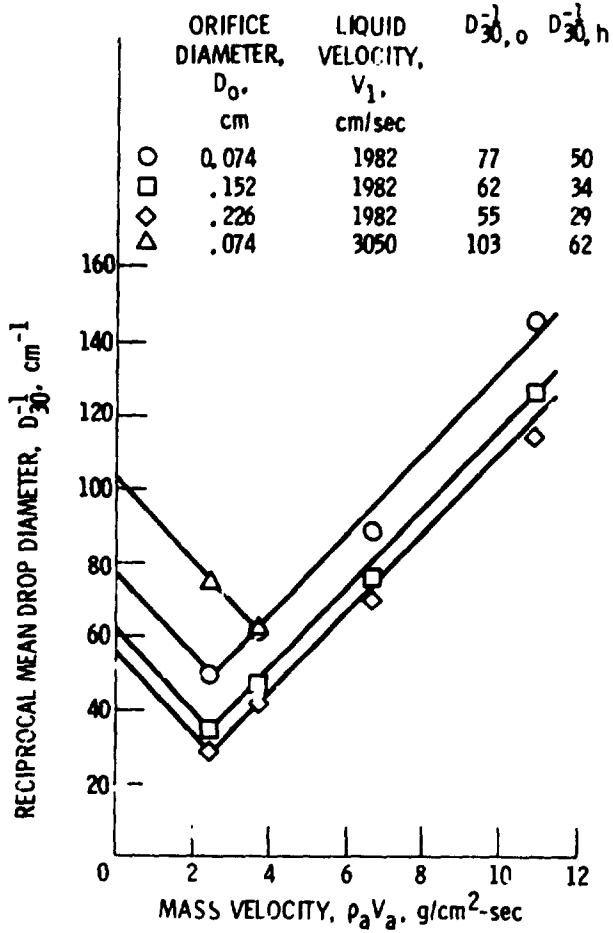

Figure 12. - Variation of reciprocal mean drop diameter, D_{30}^{-1}, with airstream mass velocity, $\rho_a V_a$, for n-heptane sheets produced by impinging jet fuel injectors.